DØNote 4366 - CONF

A DØ Search for Neutral Higgs Bosons at High $\tan\beta$ in Multi–jet Events

The DØ Collaboration
URL: http://www-d0.fnal.gov

(Dated: March 17, 2004)

A search for the production of neutral Higgs bosons in the context of the MSSM at high $\tan\beta$, using approximately 130 pb^{-1} of DØ Run II data, is presented. The analysis searches for a signal in the invariant mass spectrum of the two jets with the highest transverse energy in triple b-tagged multi-jet events. Data agree well with the Standard Model backgrounds. In the absence of evidence for a signal, the values of $\tan\beta > 80 - 120$ are excluded at 95% Confidence Level (C.L.), depending on m_A, which was studied from 90 – 150 GeV.

Preliminary Results for Winter 2004 Conferences

FIG. 1: Leading–Order Feynman diagrams showing gg, $q\overline{q}\rightarrow b\overline{b}$h production.

I. INTRODUCTION

In two–Higgs–doublet models of Electro–Weak Symmetry Breaking in general, and in the Minimal Supersymmetric extension of the Standard Model (MSSM) in particular, there are five physical Higgs states after symmetry breaking: two neutral CP–even scalars, h and H (where H is defined to be the heavier state), a neutral CP–odd scalar, A, and two charged states, $H^{\pm}$. The ratio of the vacuum expectation values of the two Higgs doublets is called $\tan\beta$. In general, the coupling of the neutral Higgs bosons to the down–type quarks, such as the b–quark, are enhanced by a factor of $\tan\beta$ relative to the Standard Model, and thus production cross–sections are proportional to $\tan^2\beta$. The Higgs bosons' widths are relatively small (compared to the di–jet mass resolution of the detector) up to very high $\tan\beta$ ($\lesssim 100$). The neutral Higgs bosons are expected to decay about 90% of the time to a pair of bottom quarks.

Using the multi–jet data taken by DØ in September 2002 – July 2003 that corresponds to an integrated luminosity of 131 pb^{-1}, we search for a peak in the di-jet invariant mass distribution of events containing three or more b–tagged jets.

LEP has excluded at 95% C.L. a light neutral Higgs for m_h<91 GeV, for all values of $\tan\beta$ [1]. CDF has excluded at 95% C.L. values of $\tan\beta$>60–100 in the MSSM for m_A ranging from the LEP lower limit up to 200 GeV, using 91 pb^{-1} of data from Run I of the Tevatron[2].

A. Higgs Bosons in the MSSM

Associated production of neutral Higgs bosons with either one or two high-p_T ($p_T > 15$ GeV) b–quarks takes place through the Leading Order (LO) process gb→bh and gg,$q\overline{q}\rightarrow b\overline{b}$h, respectively, as shown by the Feynman diagrams in Fig. 1 for the latter case. Similar diagrams exist for H and A as well.

Figure 2 shows the LO cross–sections for A and h/H production associated with a $b\overline{b}$ pair for $\tan\beta = 1.5$ and 30 at a $p\bar{p}$ collider at $\sqrt{s} = 1960$ GeV, calculated with the Hqq program [3]. (The LO cross–sections are only used here to show the general form of the production for the three neutral Higgs bosons, and how it scales with $\tan\beta$. The NLO calculations [4], which have recently become available, are used for setting limits on $\tan\beta$.) At high $\tan\beta$, the production of either the h or the H is always nearly equal to that of the A, for all m_A. Since this analysis is unable to distinguish between the h/H and the A, we will simply assume that production of the A doubles the total cross–section. At no point in parameter space is the simultaneous production of all three neutral Higgs bosons large. We assume that the cross–section for A production scales as $\tan^2\beta$, as does the cross–section for the sum of the h and H production.

The typical input parameters chosen for the MSSM Higgs sector are m_A and $\tan\beta$. Given these, the masses of the other Higgs bosons and all couplings to fermions can be derived [5]. At LO, $m_h < m_Z|cos(2\beta)|$, $m_h < m_A$, $m_H > m_A$, and $m^2_{H^{\pm}} = m^2_W + m^2_A$. However, large radiative corrections from virtual top, stop (and bottom, at high $\tan\beta$) loops extend the upper limit of m_h to about 135 GeV. The dependence of m_h and m_H on m_A is shown on the left–hand side of Fig. 3 for $\tan\beta = 30$. At high $\tan\beta$ ($\gtrsim 20$) the A is always nearly degenerate in mass with either the h or the H.

The widths, branching fractions, and masses for the neutral Higgs bosons have been calculated using the program HDECAY [6]. The widths of the neutral Higgs bosons for $\tan\beta$ of 30 are shown on the right–hand side in Fig. 3. They are smaller than the detector resolution (∼20 GeV) for $\tan\beta \lesssim 100$. When the production cross–section of either the h or H is very small, their widths are also very small. Both effects are caused by the decreased coupling of the Higgs boson to the bottom quark. All of the neutral Higgs bosons are predicted to decay to $b\overline{b}$ ∼90% of the time at high $\tan\beta$ whenever their production in association with bottom quarks is enhanced.

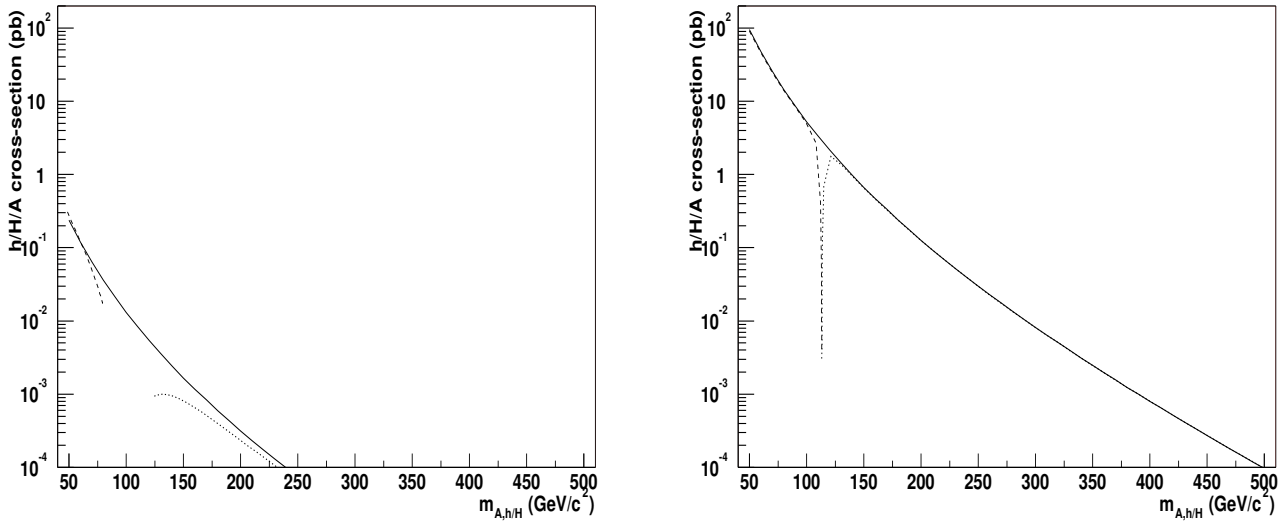

FIG. 2: Production cross–sections for neutral Higgs bosons associated with a $b\overline{b}$ pair at LO [3], for $\tan\beta$ of 1.5 (left) and 30 (right). (The A is solid, the h is dashed, and the H is dotted.)

II. DATA AND MONTE CARLO SAMPLES

A. Trigger

Due to the very high cross–section of multi–jet events and limited bandwidth at each trigger level, a specialized trigger was developed to maximize signal acceptance while remaining within rate–to–tape constrains (<4 Hz), as well as constraints at earlier trigger levels, up to moderate luminosity ($4 \times 10^{31} cm^{-2} s^{-1}$). This data set spans two trigger versions, with the first having collected about 75 pb^{-1} of integrated luminosity and the second coming online in March, 2003, collecting about 56 pb^{-1} of the data.

The first trigger version demanded four calorimeter towers with E_T>5 GeV at L1, three L2 "jets" with E_T>8 GeV and total L2 H_T (scalar sum of L2 jets with E_T>5 GeV) above 50 GeV, and three L3 jets with E_T>15 GeV. The detector $|\eta|$ coverage was up to 2.4 at L1/L2 and 3.0 at L3.

The second trigger version demanded only three calorimeter towers with E_T>5 GeV at L1, the same requirements at L2, and three L3 jets with E_T>15 GeV where two of them have E_T>25 GeV. The L3 jets used in both triggers were not corrected for non–linearity of the calorimeter or the jet energy scale. However, the jets' E_T and η were corrected for the Z position of the primary vertex, significantly sharpening the turn–on curve, as compared to the first trigger.

B. Data Selection

A total of 30.3 million events were "skimmed" from the full data sample which had one 0.5 cone jet [7] reconstructed with E_T>20 GeV and another two with E_T>15 GeV, in $|\eta|$<2.5 (uncorrected, and before any jet quality cuts), and satisfied one of the two multi–jet triggers.

Jets are then required to pass quality cuts, which help to eliminate fake jets and EM objects. Their energies are corrected back to the particle level for detector and physics effects using the standard jet energy scale factors. Typical relative correction values are +30% for data, and +20% for MC jets, with errors of about 5% (mainly systematic). Jets are also required to have $|\eta|$<2.5 and E_T>15 GeV in order to have the jet energy scale applied to them. This is also the fiducial region for b–tagging.

A b–jet can not be separated from a light–quark (or gluon) jet if it does not meet certain minimal requirements, called "taggability": each jet is required to have at least two associated tracks, within ΔR<0.5, with p_T>0.5 GeV, and $\geq$ 3 silicon tracker hits and $\geq$ 7 (0) central fiber tracker hits in the central (forward) region to be taggable. Also, each event is required to contain a primary vertex reconstructed with $\geq$ 4 tracks attached to it, in order for any of the jets in that event to be taggable. Approximately 75% of jets are taggable in data and 85% in Monte Carlo. This

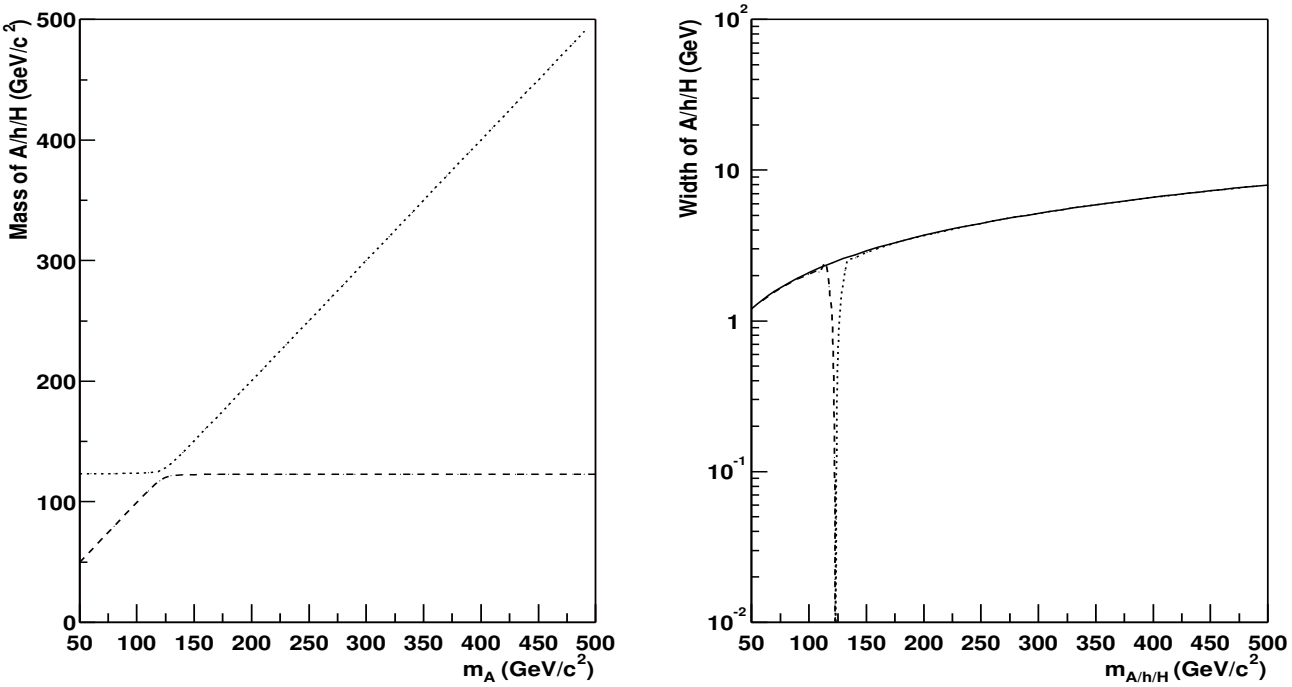

FIG. 3: Dependence on m_A of m_h and m_H (left). Total widths for neutral Higgs bosons (right). Both are for $\tan\beta$ of 30, taken from [6].

difference is taken into account in detail by the b-tagging data/MC scale factors. b–tagging was performed using the Secondary Vertex Tagger (SVT) algorithm. We used the Extra Loose definition, based on early studies. This type has the highest b–tagging efficiency, 51% on taggable jets (with $E_T >$ 35 GeV), but also the largest light-jet fake b-tagging rate, about 2%.

C. Monte Carlo

Events of the expected signals and backgrounds were generated by PYTHIA [8] or ALPGEN [9] passed through PYTHIA showering. These events were then fed through the full DØ detector simulation and reconstruction chain. Minimum bias events generated with PYTHIA were added to all generated events, Poisson distributed with a mean of 0.5 to simulate the instantaneous luminosities at which the data was taken (1–4$\times 10^{31} cm^{-2} s^{-1}$).

1. Signal

Samples of bh events (with h decaying to $b\bar{b}$) were generated for various Higgs masses, from 90 to 150 GeV, using PYTHIA. The p_T and rapidity spectra of the Higgs (for m_h = 120 GeV) were compared to those from the NLO calculation [4]. The shapes agree well, indicating that the PYTHIA kinematics are approximately correct. To further improve the agreement between PYTHIA and NLO, the PYTHIA events were re–weighted, to match the NLO Higgs p_T spectrum. There was a 13% reduction in the overall signal efficiency caused by the re–weighting.

bbh events (with h decaying to $b\bar{b}$) were also generated, for comparison with the bh events. This calculation is generally believed to be more reliable when 4 high–p_T b–jets are to be tagged in each event. A prescription was tried which matched the two samples (bh and bbh) by the p_T of the lowest p_T spectator b-quark in each event. The kinematics and normalization were similar to within 5% when either the matching prescription, bh only, or bbh only was used. We chose to rely on the bh signal events only, re–weighted using the procedure described above, which is the most conservative choice.

2. Heavy–flavor Multi–jet

Multi–jet production, such as $p\bar{p}\rightarrow$3j, 4j, $b\bar{b}$j, $b\bar{b}$jj, and $b\bar{b}b\bar{b}$ (where j represents a light quark (u,d,s), charm quark, or gluon jet) is very difficult to model correctly. Fortunately, several leading–order matrix element generators are now able to produce unweighted events of these complicated processes. ALPGEN v1.2, was used to generate events of $b\bar{b}$j, $b\bar{b}$jj, and $b\bar{b}b\bar{b}$. However, in the end, the multi–jet backgrounds were always estimated from data.

3. Other Backgrounds

Several other potential sources of background were also simulated with PYTHIA: inclusive $p\bar{p}\rightarrow t\bar{t}$, $p\bar{p}\rightarrow$Z($\rightarrow b\bar{b}$) (+jets), and $p\bar{p}\rightarrow$Zb $\rightarrow b\bar{b}$b. Cross–sections of 7 pb, 1.18 nb, and 40 pb [12] were assumed, respectively.

III. ANALYSIS

A. Background Estimation

Of all Standard Model processes, multi–jet production is the major source of background. Also significant are the Z($\rightarrow b\bar{b}$) (+jets) and $t\bar{t}$ processes. The multi–jet backgrounds are, in the end, normalized outside the signal search region in the triple b–tagged data. However, we attempt to model the multi–jet backgrounds in Monte Carlo as a crosscheck and to have some feel for what physical processes make up the backgrounds.

The invariant mass distribution of the leading two (E_T) jets in the double b–tagged data (events with 2 or more b–tags) is fit to a sum of backgrounds. The expected signal contribution to the double b–tagged data is negligible and does not affect the normalizations of the backgrounds. The multi–jet background is divided into three categories, for the purpose of accounting and for comparison with the simulations. The first category, multi–jet fakes, is light multi–jet production, where two or more jets are either light–quark or gluon jets that have been falsely identified as b–jets or possibly gluon–jets where the gluon has split into b or c–quarks. Heavy–flavor (HF) multi–jet production (either $b\bar{b}$jj or $b\bar{b}$j, depending on whether 3 jet states are allowed as well as 4 jet states) has two real b–jets, both of which have been b–tagged. We comment on the contribution of $c\bar{c}$j(j) below. The last category contains all other backgrounds, such as $b\bar{b}b\bar{b}$, Z($\rightarrow b\bar{b}$) (+jets), and $t\bar{t}$.

The multi–jet fakes are estimated from data. Using the full data sample, the probability of b–tagging a jet is measured, as a function of the E_T of the jet, in three different $|\eta|$ bins. In the following, this function will be called the "fake–tag" function, although it is understood to have some contamination at this point from true HF events in the data sample from which it was derived, and gluon jets where the gluon has split into a $b\bar{b}$ or $c\bar{c}$ pair. The contribution to the fake–tag function from isolated bottom and/or charm jets is removed by estimating the fraction of $b\bar{b}$jj events in the full multi–jet data sample (1.2%) from an initial fit to the double b–tagged data. The fake–tag function is lowered by 7.8% by this correction. This corrected fake–tag function is then used to estimate the multi–jet fakes contribution by applying it to every jet in the full sample. The probability for an event to have two or more fake–tags is used as the probability for that event to enter the multi–jet fakes distribution.

The b–tagging used in this analysis is unable to distinguish contributions from bottom and charm events. However, the efficiency for tagging a charm–jet is about 1/4 of that for tagging a bottom–jet. Therefore, when two b–tags are required, the fraction of $c\bar{c}$j(j) events relative to $b\bar{b}$j(j) events will be a factor of $\sim 4^2 = 16$ times lower after tagging than it was before. We have estimated the fractions of $c\bar{c}$jj to $b\bar{b}$jj prior to b–tagging using the MADGRAPH Monte Carlo generator [10]. The $c\bar{c}$jj cross–section was estimated to be 3240±174 pb, only 22% higher than the $b\bar{b}$jj cross–section, using the same generator–level cuts. We therefore estimate the contribution of $c\bar{c}$j(j) in the double b–tagged data sample to be $\sim 1.22/16 = 8\%$ of the events. Thus, when we refer to $b\bar{b}$jj normalization, it should be understood that a small fraction, approximately 8% is really from the $c\bar{c}$jj process.

The normalization of the HF multi–jet processes ($b\bar{b}$jj and $b\bar{b}b\bar{b}$) is left as a free parameter in the fit. The ratio of the two HF multi–jet cross–sections is taken from ALPGEN. The Z($\rightarrow b\bar{b}$) (+jets) and $t\bar{t}$ backgrounds are fixed to the integrated luminosity times their assumed cross–sections. The fit of the double b–tagged data is shown in Fig. 4, with cuts optimized for events with 4 or more jets and m_h=120, from Table I. After corrections for $c\bar{c}$jj events, the HF multi–jet processes are only a factor of 1.14 ± 0.02 (stat) higher in data than predicted by ALPGEN, which is much better agreement than seen in previous comparisons [11]. The data agrees well with the shape of the estimated background over the entire invariant mass region.

To estimate the triple b–tagged background, the fake–tag function is applied to the non–b–tagged jets in each event in the double b–tagged data sample, and the probability is calculated for each of the events to have three or more b–tags. We will refer to this parameterization of the background as the "triple b–tag estimation". This of course

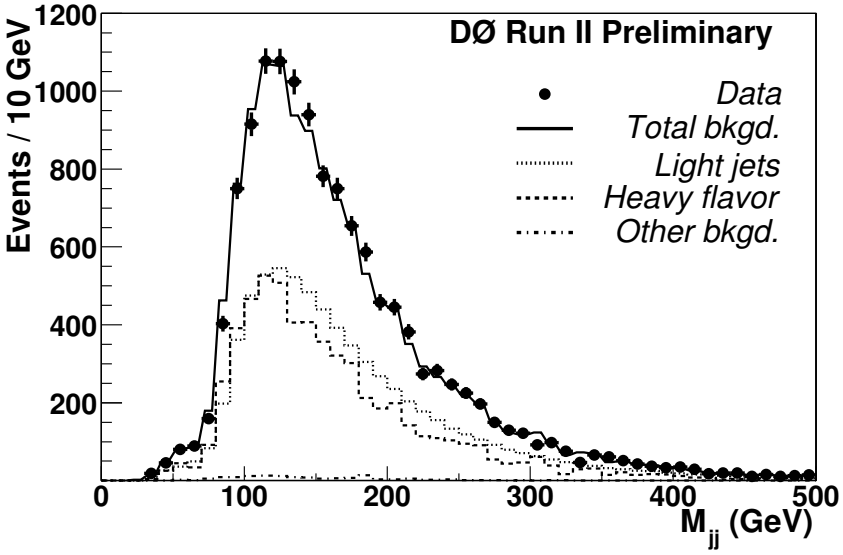

FIG. 4: Final fit of the double b–tagged data's two leading jet invariant mass spectrum, after fake–tag parameterization correction, to a sum of backgrounds: multi–jet fakes from data (dotted), ALPGEN $b\bar{b}$jj MC (dashed), and other small backgrounds (Z($\rightarrow b\bar{b}$) (+jets), $t\bar{t}$, and ALPGEN $b\bar{b}b\bar{b}$) (dashed–dotted). The cuts correspond to those optimized for n_j^{min}=4 and m_h=120, from Table I.

neglects the contribution from processes which have more than two real b–jets, such as $b\bar{b}b\bar{b}$ and Z($\rightarrow b\bar{b}$)$b\bar{b}$. However, the shape of these backgrounds is seen to be very similar to the double b–tagged spectrum.

The overall background normalization is determined by fitting the triple b–tagged invariant mass distribution outside the signal region ($\pm 1\sigma$ of the Gaussian fit to the expected signal) with the triple b–tag estimation, derived from the double b–tagged data using the fake–tag function. The resulting fit using this method of background normalization is shown in Fig. 5 for n_j^{min}=3 and m_h = 120 GeV(see Table I).

B. Optimization

The analysis is optimized using Monte Carlo. It was verified above that the shapes of the simulated backgrounds accurately model both the double and triple b–tagged data. Thus it is safe to assume that a fairly optimal set of analysis cuts can be achieved by using the simulated backgrounds alone. We have no choice but to use simulated signal events.

The expected signal production limit, as calculated using the methods discussed below, has been optimized. A separate optimization is performed for two values of n_j^{min}, the minimum number of jets allowed in the final state, 3 and 4. Beginning with a basic and loose set of analysis cuts, one parameter is optimized at a time, by varying the parameter, deriving the expected 95% C.L. limit and choosing the value of the parameter which minimizes the tan β limit. The parameters are also optimized separately for each m_h studied (in addition to the two possible n_j^{min}).

The resulting optimized values for each m_h and for n_j^{min}=3,4 are shown in Table I. The optimal cuts are approximately independent of the Higgs mass and the number of jets allowed. Harder E_T cuts of 60 and 40 GeV are used for the leading and next–to–leading jets and slightly tighter η cuts, for m_h=150 GeV. Also, 5 jet final states are allowed in the n_j^{min}=4 channel for all but the lightest Higgs mass studied. No events were considered with more than 5 jets in the n_j^{min}=4 channel, or 4 jets in the n_j^{min}=3 channel, since our Monte Carlo, which relies on PYTHIA showering, may not be reliable beyond one extra jet.

C. Acceptance Systematics

The errors from sources which affect the signal acceptance are added in quadrature, and are shown in Table II. The procedure used to normalize the simulated signal events to the NLO cross–sections and p_T spectra is only an approximation to reproducing the full NLO kinematics, thus an error of half the re–weighting correction is assigned,

Signal (GeV)	$E_T{}^1$(GeV)	$E_T{}^2$(GeV)	$E_T{}^3$(GeV)	$\|\eta\|_j$	n_j^{max}
n_j^{min}=4, m_h=100	40	35	15	2.5	4
n_j^{min}=4, m_h=120	45	35	15	2.5	5
n_j^{min}=4, m_h=150	60	40	15	2.0	5
n_j^{min}=3, m_h=100	45	35	15	2.5	4
n_j^{min}=3, m_h=120	45	35	15	2.5	4
n_j^{min}=3, m_h=150	60	40	15	2.0	4

TABLE I: Optimized analysis cuts for each m_h studied and for both n_j^{min} cases, 3 and 4.

Signal (GeV)	NLO/LO (%)	Trig (%)	Resolution (%)	JES (%)	Jet ID (%)	B–tag (%)	Total (%)
n_j^{min}=4, m_h=100	5	9	8.0	20	3.8	13.5	27.7
n_j^{min}=4, m_h=120	5	9	12.0	16	3.4	13.5	26.5
n_j^{min}=4, m_h=150	5	9	11.9	13	3.5	13.8	24.9
n_j^{min}=3, m_h=100	5	9	7.5	12	3.7	13.5	22.4
n_j^{min}=3, m_h=120	5	9	12.5	7.5	3.5	13.2	22.5
n_j^{min}=3, m_h=150	5	9	12.8	3.4	3.6	13.4	21.8

TABLE II: The errors from each source (in percent), which are added in quadrature to give the total errors on acceptance.

5%.

The overall trigger efficiency is subject to errors coming from the limited statistics of the data samples used to measure the trigger efficiencies, the inaccuracy with which the parameterized turn–on curves represent the true turn–ons, and the limitations of the assumptions made about the independence of jets at the trigger level. The total trigger uncertainty from these sources is estimated to be ±9%. Typical errors involved in the closure–tests (the average difference between the predicted trigger rate and the observed trigger rate) were about 5%.

If the jet energy resolution is different in data than in the Monte Carlo, more or less signal events would be included under a Gaussian peak in reality than was assumed. The reported uncertainties for the Monte Carlo and data jet energy resolutions are added in quadrature, and the resulting uncertainty in the difference between data and Monte Carlo resolution is 8% for jets with E_T between 40 and 60 GeV, averaged over the η ranges weighted by the largely central Higgs jet η spectrum. Since the width of the signal distributions is approximately $\sqrt{2}\sigma$, where σ is the jet energy resolution, the width of the fitted signal distributions will be assigned an uncertainty of $\sqrt{2}$ times the jet energy resolution uncertainty, or 12%. The acceptance error is then estimated from the fractional change in signal acceptance when a Gaussian peak fit to the signal has its width changed by ±12%.

To calculate the systematic error resulting from the jet energy scale, the entire analysis has been repeated, changing the jet energy scale up and down by $\pm 1\sigma$ of its uncertainty. The correlation between the error on the Higgs peak widths, from the jet energy resolution error, and the jet energy scale error was found to be negligible, and we thus add the two errors in quadrature.

The jet reconstruction efficiency has been measured both in Monte Carlo and in data, as a function of E_T. Each jet in the simulation was adjusted for the difference between the two efficiencies, but the error on that difference correction remains. The error is estimated by taking the $\pm 1\sigma$ values for the jet reconstruction efficiencies and repeating the full analysis.

The uncertainty on signal acceptance due to b–tagging is represented by the error on the data–to–Monte Carlo b–tagging scale factor. The analysis was run using the $\pm 1\sigma$ scale factors, and the difference in accepted signal fraction was measured.

The absolute value of the integrated luminosity that the data sample corresponds to has an uncertainty of 10%.

D. Background Systematics

There is a statistical error associated with the uncertainty in the normalization of the background, as fit outside the signal region. Additional systematic uncertainty arises from the shape of the distribution not being modelled perfectly, which can be estimated from the χ^2/NDF of the background normalization fit. The statistical error is multiplied by the $\sqrt{\chi^2/NDF}$ for each m_h.

Signal (GeV)	3 b–tag Fit (%)	Fake–tag Fit (%)	Total Error (%)
n_j^{min}=4, m_h=100	8.2	8	11.5
n_j^{min}=4, m_h=120	7.1	8	10.7
n_j^{min}=4, m_h=150	6.7	8	10.0
n_j^{min}=3, m_h=100	7.8	7	10.0
n_j^{min}=3, m_h=120	6.9	7	9.8
n_j^{min}=3, m_h=150	6.6	7	9.6

TABLE III: The errors on the background normalization, measured via both of the methods investigated, and the total error assigned, for each m_h and number of minimum jets allowed.

Signal (GeV)	Kinematic (%)	Trigger (%)	B-tagging (%)	Total (%)
n_j^{min}=4, m_h=100	1.25	69	23	0.20
n_j^{min}=4, m_h=120	2.40	71	21	0.36
n_j^{min}=4, m_h=150	3.92	79	20	0.63
n_j^{min}=3, m_h=100	4.75	59	17	0.48
n_j^{min}=3, m_h=120	8.55	62	17	0.89
n_j^{min}=3, m_h=150	13.2	71	16	1.5

TABLE IV: The acceptance for signal of each set of analysis cuts, for each m_h, in the 3 and 4 jet cases.

Another method of calculating the uncertainty in the background normalization is to use the statistical uncertainty of the fake–tag parameterization fit multiplied by its $\sqrt{\chi^2/NDF}$, since this function is used to propagate the shape of the double b–tagged data to the triple b–tagged data. The results of both methods and the total errors used for the background normalization are listed in Table III, as a function of m_h.

E. Limit Setting Method

The implementation of the MCLimit routines [13] in Root version 3.05/07 were used to set limits on signal production. The full leading di–jet invariant mass histograms for the triple b–tagged events in data, simulated signal, and normalized background were input. The value of $\tan\beta$ was varied, starting at 50, either up or down until the C.L. for signal was <5%. The signal histogram was scaled by $\tan^2\beta$. The increased width of the Higgs bosons at high $\tan\beta$ was simulated by smearing the Higgs boson resonance in each event, by systematically changing the E_T of the jets which make up the Higgs boson mass peak by a Gaussian function with a width set to that of the Higgs boson. Systematic uncertainties on the signal acceptance, background normalization, and luminosity were taken into account during limit setting.

IV. RESULTS

The cuts made in this analysis can be summarized as taking place in three sets: the trigger level, the kinematic cuts (E_T, η, n_j, etc.), and b–tagging. Table IV shows the acceptance of each set of cuts made in the analysis, for each m_h. The kinematic cuts are satisfied more often for heavier Higgs bosons. The trigger efficiency rises slightly as a function of the mass of the Higgs. The trigger efficiency is also slightly better for the n_j^{min}=4 than the n_j^{min}=3 cuts, since there is frequently an extra jet to trigger on. b–tagging efficiencies are approximately independent of Higgs mass, but are higher when there is the fourth b–jet available for tagging.

Figure 5 shows the data, background, and Higgs mass peak at the exclusion limit, for m_h = 120 GeV. For each Higgs mass studied, the $\tan\beta$ limit was derived, and they are listed in Table V. Better limits are obtained for the n_j^{min}=3 cuts, so these are plotted in Fig. 6. Three data points around the di-jet invariant mass of 160 GeV are higher than the expected background. However, a Gaussian fit to a signal plus background hypothesis yields a width too narrow to be compatible with the di–jet mass width of signal, which is about 25 GeV for m_h=160 GeV (not taking into account the additional effects of the natural width of the Higgs at high $\tan\beta$).

Signal (GeV)	Higgs Width (GeV)	Expected $\tan\beta$ Limit	$\tan\beta$ Limit
n_j^{min}=3, m_h=90	8	91	96
n_j^{min}=3, m_h=100	10	96	97
n_j^{min}=3, m_h=120	15	109	109
n_j^{min}=3, m_h=150	45	138	140

TABLE V: The width of the Higgs at the $\tan\beta$ value excluded at 95% C.L., the expected 95% C.L. $\tan\beta$ limit, and the 95% C.L. $\tan\beta$ limit set from data.

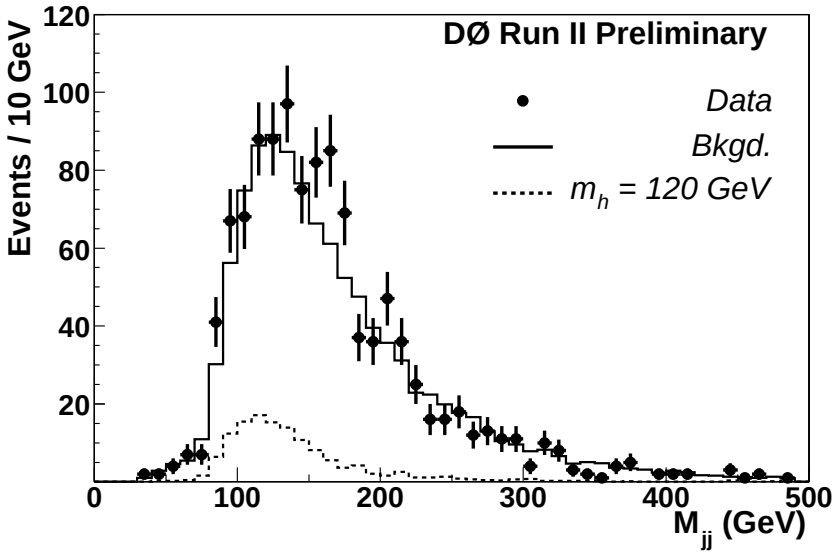

FIG. 5: The triple b–tagged data, estimated background, and Higgs signal at the 95% C.L. exclusion limit, after the addition of the Higgs width, for n_j^{min}=3 and m_h = 120 GeV.

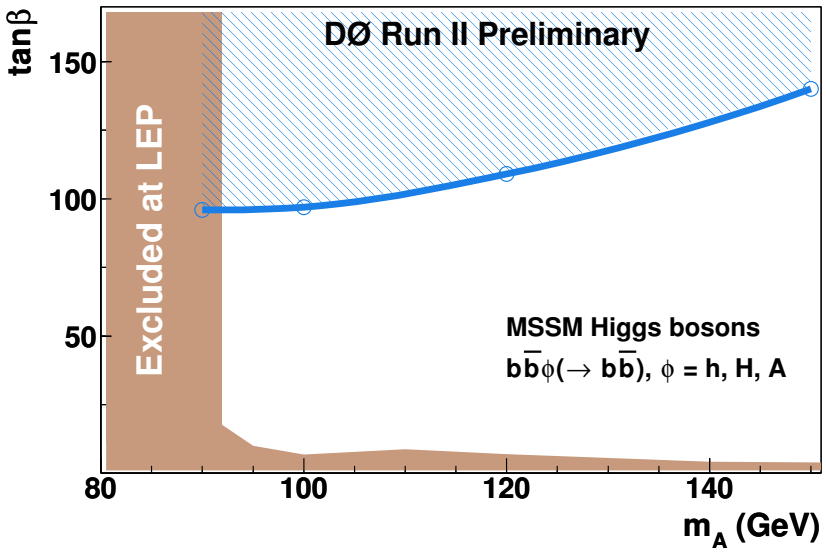

FIG. 6: The 95% C.L. lower limit on $\tan\beta$ set as a function of m_A (thick, blue), for the n_j^{min}=3 cuts and including the effects of the Higgs boson widths at high $\tan\beta$. The top hatched area indicates the excluded side of the line, and the shared area indicates the LEP limits.

Acknowledgments

We thank the staffs at Fermilab and collaborating institutions, and acknowledge support from the Department of Energy and National Science Foundation (USA), Commissariat à L'Energie Atomique and CNRS/Institut National de Physique Nucléaire et de Physique des Particules (France), Ministry for Science and Technology and Ministry for Atomic Energy (Russia), CAPES, CNPq and FAPERJ (Brazil), Departments of Atomic Energy and Science and Education (India), Colciencias (Colombia), CONACyT (Mexico), Ministry of Education and KOSEF (Korea), CONICET and UBACyT (Argentina), The Foundation for Fundamental Research on Matter (The Netherlands), PPARC (United Kingdom), Ministry of Education (Czech Republic), A.P. Sloan Foundation, Civilian Research and Development Foundation, Research Corporation, Texas Advanced Research Program, and the Alexander von Humboldt Foundation.

---

[1] LEP Higgs Working Group (July 2001), Note/2001-04, hep-ex/0107030.
[2] CDF Collaboration, Phys.Rev.Lett. 86 (2001) 4472-4478.
[3] M. Spira, "Higgs Boson Production and Decay at the Tevatron", hep-ph/9810289.
[4] J. Campbell, R.K. Ellis, F. Maltoni, S. Willenbrock, "Higgs-Boson Production in Association with a Single Bottom Quark", Phys.Rev.D67 (2003) 095002, hep-ph/0204093 v2.
[5] The Higgs Working Group: Summary Report (2001), hep-ph/0203056, pages 10-28.
[6] M. Spira, "HDECAY", hep-ph/9704448, http://people.web.psi.ch/spira/hdecay/.
[7] G. Blazey, et. al., "Run II Jet Physics: Proceedings of the Run II QCD and Weak Boson Physics Workshop", hep-ex/0005012.
[8] T. Sjstrand, P. Edn, C. Friberg, L. Lnnblad, G. Miu, S. Mrenna and E. Norrbin, Computer Phys. Commun. 135 (2001) 238 (LU TP 00-30, hep-ph/0010017).
[9] M.L. Mangano, M. Moretti, F. Piccinini, R. Pittau, A. Polosa, "ALPGEN, a generator for hard multiparton processes in hadronic collisions", JHEP 0307:001,2003, hep-ph/0206293.
[10] F. Maltoni, T. Stelzer, "MADEVENT: Automatic Event Generation with MADGRAPH", JHEP 0302:027,2003, hep-ph/0208156.
[11] A. Annovi, P. Giannetti, "B Production in Multijet Events", Matrix Element / MC Tuning Workshop, Fermilab, Oct. 4, 2002, http://cepa.fnal.gov/CPD/MCTuning/event_gen_2002.pdf.
[12] J. Campbell, R. K. Ellis, F. Maltoni, S. Willenbrock, "Associated Production of a Z Boson and a Single Heavy-Quark Jet", hep-ph/0312024.
[13] T. Junk, "Confidence Level Computation for Combining Searches with Small Statistics", Nucl.Instrum.Meth. A434 (1999) 435-443, hep-ex/9902006.